Fujikawa and Yamada
BioMedical Engineering OnLine (2024) 23:94
https://doi.org/10.1186/s12938-024-01284-2

BioMedical Engineering OnLine

RESEARCH Open Access

In vivo video microscopy of the rupturing process of thin blood vessels to clarify the mechanism of bruising caused by blunt impact: an animal study

Tatsuo Fujikawa[1*] and Yoji Yamada[2]

*Correspondence:
fujikawa.tatsuo@nihon-u.ac.jp

[1] Department of Mechanical Engineering, College of Engineering, Nihon University, 1 Nakagawara, Tokusada, Tamuramachi, Koriyama 963-8642, Japan
[2] Department of Mechanical System Engineering, Nagoya University, Furo-Cho, Chikusa-Ku, Nagoya 464-8603, Japan

Abstract

Background: The thresholds of mechanical inputs for bruising caused by blunt impact are important in the fields of machine safety and forensics. However, reliable data on these thresholds remain inadequate owing to a lack of in vivo experiments, which are crucial for investigating the occurrence of bruising. Since experiments involving live human participants are limited owing to ethical concerns, finite-element method (FEM) simulations of the bruising mechanism should be used to compensate for the lack of experimental data by estimating the thresholds under various conditions, which requires clarifying the mechanism of formation of actual bruises. Therefore, this study aimed to visualize the mechanism underlying the formation of bruises caused by blunt impact to enable FEM simulations to estimate the thresholds of mechanical inputs for bruising.

Methods: In vivo microscopy of a transparent glass catfish subjected to blunt contact with an indenter was performed. The fish were anesthetized by immersing them in buffered MS-222 (75–100 mg/L) and then fixed on a subject tray. The indenter, made of transparent acrylic and having a rectangular contact area with dimensions of 1.0 mm × 1.5 mm, was loaded onto the lateral side of the caudal region of the fish. Blood vessels and surrounding tissues were examined through the transparent indenter using a microscope equipped with a video camera. The contact force was measured using a force-sensing table.

Results: One of the processes of rupturing thin blood vessels, which are an essential component of the bruising mechanism, was observed and recorded as a movie. The soft tissue surrounding the thin blood vessel extended in a plane perpendicular to the compressive contact force. Subsequently, the thin blood vessel was pulled into a straight configuration. Next, it was stretched in the axial direction and finally ruptured.

Conclusion: The results obtained indicate that the extension of the surrounding tissue in the direction perpendicular to the contact force as well as the extension of the thin blood vessels are important factors in the bruising mechanism, which must be reproduced by FEM simulation to estimate the thresholds.

Keywords: Safety of machinery, Forensics, Non-accidental injuries, Internal bleeding, Soft tissue injury, Transparent glass catfish

Introduction

To ensure the safety of individuals while operating machinery, the thresholds of mechanical inputs for bruising are collectively regarded as a major component of safety criteria [1–3]. Machinery such as robots that work in collaborative environments with humans should be designed to maintain the values of mechanical inputs, e.g., contact force and contact pressure, lower than the thresholds during contact with human body parts to prevent bruising [1, 2]. Behrens et al. [3] demonstrated that the probability of bruise occurrence is a function of three mechanical inputs, namely the contact force, contact pressure, and energy density, although it was unclear which variables were most important. Contact force and contact pressure are the maximum values in impulsive data. The energy density is a parameter representing the impulse, which is evaluated by integrating the contact pressure with respect to the deformation of impacted body parts. The mechanical aspects of bruise formation are also important in the field of forensics, as they provide clinical evidence for inspecting non-accidental injuries, including abuse [4–7]. Inspection of the bruising conditions by considering the mechanical inputs provides information for identifying the type of impact exerted on victims.

However, reliable data on the mechanical input thresholds for bruising are still inadequate owing to a lack of in vivo data. Although in vivo experiments are crucial for investigating the occurrence and type of bruising, as they are formed on living soft tissues, experiments involving live human participants are limited owing to ethical concerns. Desmoulin and Anderson [5] investigated the bruising of human legs impacted by a sphere-shaped impactor, and Povse [2] examined mild contusions in human forearms impacted by the end effectors of a robot and compared the mechanical inputs and the occurrence of injuries. However, they did not clearly determine the thresholds because only one human subject participated in each study. Behrens et al. [3] conducted the first experiment that provided reliable human data on bruising. They performed impact tests on five body parts of 24 human participants using three types of impactors. The results indicated that the thresholds varied depending on the parts of the body and the type of impactor. Therefore, experiments on multiple parts of the human body and the various types of impactors are needed to obtain sufficient data on the thresholds.

Huang et al. [8], Tang et al. [9], Grosse et al. [10], and Higuchi et al. [11] tried to use finite-element method (FEM) simulations to investigate the occurrence of bruises. Accurate reproduction of the bruising mechanism by simulations should compensate for the lack of experimental data by estimating the thresholds at various conditions. To achieve this, the following information on the mechanism of the formation of actual bruises must be clarified: (1) failure mode of thin blood vessels, for example, tensile failure in its axial direction, shear failure, or crushing; (2) deformation process of thin blood vessels, for example, curved blood vessels rupture with or without pre-rupture straightening; (3) effect of surrounding tissue, such as whether the deformation of the blood vessel is strongly affected by that of the surrounding tissue or is almost independent; and (4) deformation of the surrounding tissue, such as whether it extends in a direction perpendicular to the compression, as predicted by a simple contact model. The purpose of this

study is to obtain the information that enables the simulation to estimate the thresholds of mechanical inputs for bruising.

A bruise is defined as "a hurt or injury to the body by a blunt or heavy instrument causing discoloration but no laceration of the skin [12]" and "consists of blood escaping from ruptured capillaries and small veins, spreading into the surrounding tissue." [6] Therefore, the rupture of thin blood vessels caused by blunt impact is an essential aspect of this mechanism. Although the mechanical rupture of thin blood vessels has been discussed in several studies, it has not been described comprehensively. West and Mathieu-Costello [13] discussed the hoop failure process for capillary walls. This rupture mechanism is applicable to the rupture of blood vessels caused by an increase in blood pressure but not to that caused by blunt impact. Deane et al. [14] investigated rabbit soft tissues sliced from specimens that underwent impact experiments and reported that erythrocytes released from damaged blood vessels were found not only immediately beneath the area of impact but also in the deeper region where the muscle is compressed against the bone. Barington and Jensen [15] found that the number of neutrophils in porcine subcutaneous tissues sliced from specimens after impact increased with increasing contact force. Fujikawa et al. [16, 17] investigated porcine soft tissues sliced from specimens after impact and reported that the probability of erythrocytes releasing from damaged blood vessels increased with increasing contact pressure. However, they did not describe the rupturing process of thin blood vessels because their investigation was conducted after the contact. In this study, an investigation was conducted during contact to capture the process.

This study aimed to visualize the process of rupturing thin blood vessels caused by blunt contact as an essential component of the bruising mechanism. While visualization of the process during dynamic contacts is desirable, quasi-static contact was investigated as the first step in this study. The effect of the mass and viscosity of the impacted body part is smaller in quasi-static experiments than in dynamic impact, and consequently, the same contact force generates a larger strain. Therefore, the threshold measured in quasi-static experiments cannot be applied to dynamic impact. However, the process whereby a contact force causes strain and damages blood vessels is thought to be qualitatively the same for quasi-static experiments and dynamic impact. The dynamic threshold should be estimated by simulating this process while considering the mass and viscosity of the impacted body part. In such simulations, the mass is introduced as the density of the finite elements, and the viscosity is represented by Maxwell's model [11]. In vivo microscopy of thin blood vessels during quasi-static contact between the surrounding soft tissue and a transparent indenter was performed. Blood vessels in the surrounding tissues are not visible under normal conditions, and confocal laser microscopy [18] is difficult to apply to investigations using a transparent indenter because the indenter interferes with the path of the laser beam. Although fluorescence microscopy [19] is widely used to image blood vessels, the contour of the observed vessel is not clear enough to capture the rupture because the blood vessel radiates light. Steffensen et al. [20] proposed the use of transparent glass catfish for the in vivo investigation of blood vessels. In the present study, transparent glass catfish, which has transparent soft tissues in its long caudal region, was used. Furthermore, this species does not possess scales. Therefore, it helps appropriately reproduce the effect of blunt contact on the human skin, and the blood

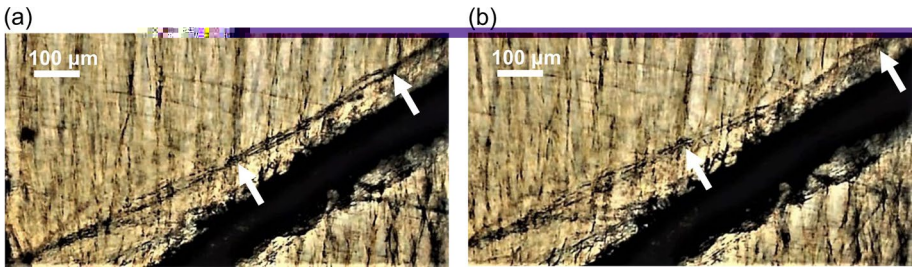

Fig. 1 Tensile rupture of a thin blood vessel. The section between the two arrows in **a** ruptured in **b**, as observed in specimen #200526-05 at a contact force of 0.28 N. A total of 5 μL/gBW of eosin (1 mg/mL) is injected into the caudal vein. The top- and left-hand sides of the images represent the anterior and ventral sides of the fish, respectively. The thick, black object is the hemal spine. The image contrast is enhanced at the same level for both images

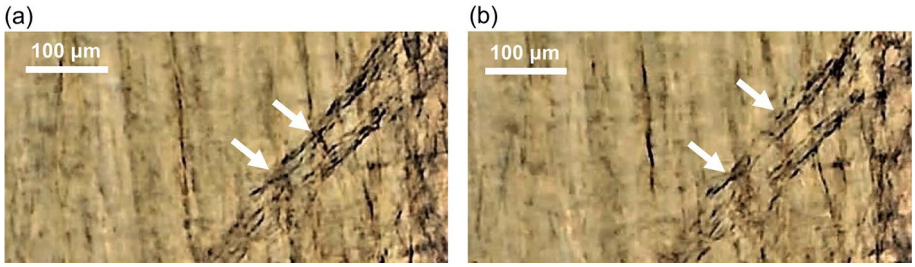

Fig. 2 Tensile rupture of a thin blood vessel. The section between the two arrows in **a** ruptured in **b**, as observed in specimen #201109-01 at a contact force of 0.48 N. A total of 6 μL/gBW of eosin (10 mg/mL) is injected into the caudal vein. The top- and left-hand sides of the images represent the anterior and ventral sides of the fish, respectively. The image contrast is enhanced at the same level for both images

vessels are visible through the transparent tissues. Fujikawa and Yamada [21] developed a technique to induce internal bleeding in a transparent glass catfish during the microscopic examination of blood vessels. This technique was used in the present study to investigate the rupturing process of thin blood vessels caused by blunt contact.

Results

Tensile rupture of thin blood vessels

The tensile rupture of thin blood vessels was observed and recorded as movies in two specimens. The movies of specimens #200526-05 and #201109-01 are shown in Additional files 1 and 2, respectively. The areas where the rupture was observed are enlarged and captured from the movie files in Figs. 1 and 2. The vessels immediately before the rupture are shown in Figs. 1a and 2a. The parts of the vessels between the pairs of arrows in Figs. 1a and 2a were stretched owing to the deformation of the surrounding tissues and ruptured, as shown in Figs. 1b and 2b, under the action of contact forces of 0.28 and 0.48 N, respectively.

Deformation of thin blood vessels and surrounding tissues before rupture

The deformation process of the thin blood vessels and surrounding tissues during contact was recorded as Additional files 3 and 4 in the same specimens as those in Additional files 1 and 2. Typical images in specimen #200526-05 are illustrated in Fig. 3.

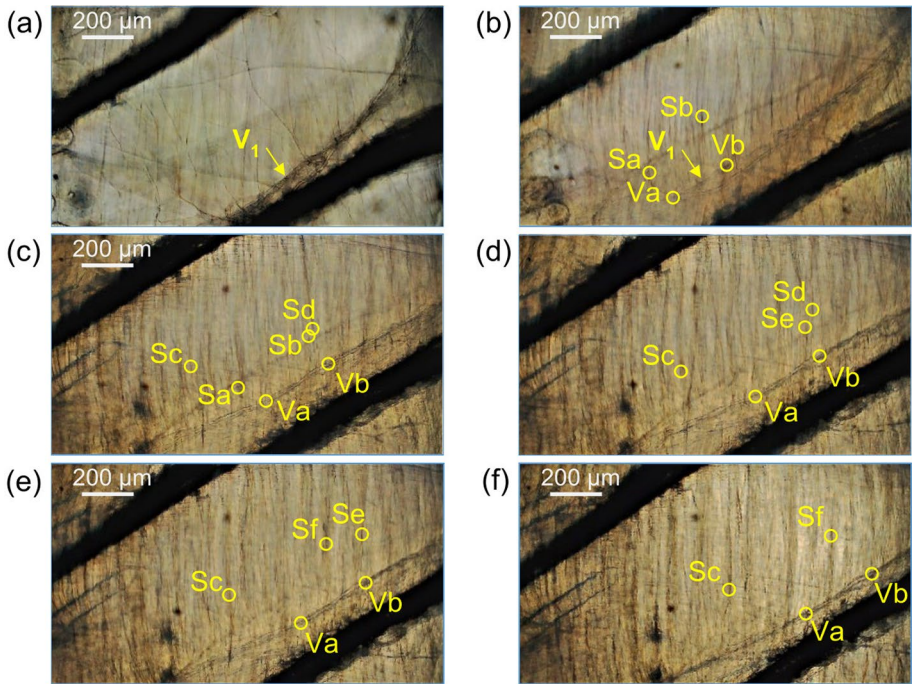

Fig. 3 Deformation of thin blood vessels and surrounding tissue. The vessels and surrounding tissue were subjected to contact forces of **a** 0.00, **b** 0.02, **c** 0.13, **d** 0.16, **e** 0.19, and **f** 0.28 N immediately before rupturing in specimen #200526-05. The anterior and ventral sides of the fish are located on the top- and left-hand sides of the images, respectively. The thick black objects are the hemal spines

The ruptured vessel shown in Fig. 1 and Additional file 1 is denoted as V_1 in Fig. 3a, b. Compared with the case of no contact force (Fig. 3a), a contact force of 0.02 N (Fig. 3b) resulted in vessel V_1 being pulled into a straighter configuration. In addition, the deformation of the vessel caused by further increasing the contact force up to 0.28 N immediately before rupture is shown in Fig. 3c–f. Points Va and Vb indicate specific points on the vessel on both sides of the ruptured part. The distance between points Va and Vb increased from 0.24 mm in Fig. 3b to 0.30 mm in Fig. 3f as the contact force increased.

Points Sa and Sb in Fig. 3b, c indicate specific points on the tissue surrounding the vessel. The distance parallel to the thin blood vessel between points Sa and Sb also increased from 0.29 mm in Fig. 3b to 0.34 mm in Fig. 3c as the contact force increased. Although points Sa and Sb vanish in Fig. 3d, another pair of points, Sc and Sd, becomes visible on the surrounding tissue in Fig. 3c, d. In addition, the distance between these points increases from 0.48 to 0.50 mm with an increase in the contact force. While the distance between points Sc and Se on the surrounding tissue (0.56 mm) in Fig. 3d has not visibly increased, as shown in Fig. 3e, the distance between points Sc and Sf on the surrounding tissue in Fig. 3e has increased from 0.42 to 0.45 mm, as shown in Fig. 3f, immediately before rupturing.

A similar deformation process of the thin blood vessel and surrounding tissue during contact was observed in specimen #201109-01.

The surrounding tissue was extended perpendicular to the contact force when it compressed in the direction of the contact force. The stretch ratio perpendicular to the contact force is approximated by the function $1/\sqrt{\lambda_z}$ of the ratio of compression

λ_z in the direction of the contact force when the deformation is approximated by a simple uniform compression with a uniformly loaded contact force; the anisotropy of the surrounding tissue is small; and the Poisson's ratio is close to 0.5. The ratio of compression λ_z is defined as

$$\lambda_z = h/h_0, \tag{1}$$

where h and h_0 are the thicknesses of the specimen during compression and under the initial condition, respectively. h and h_0 were measured by the displacement sensor during the experiments.

In Fig. 4a, the ratio of the stretch perpendicular to the contact force approximated by $1/\sqrt{\lambda_z}$ for specimen #200526-05 was compared to the actual stretch ratio of the blood vessel and surrounding tissue calculated from the length measured on Fig. 3 using formulas (2)–(4). The condition when Fig. 3b was captured, where the vessel was pulled into a straight configuration, was defined as the initial condition. As an example, the application of formulas (2)–(4) to the surrounding tissue yielded 0.34 mm for the distance l_{x1} between points Sa and Sb in Fig. 3c and 0.29 mm for the distance l_{x0} between points Sa and Sb in Fig. 3b. The values estimated in the same manner for specimen #201109-01 are shown in Fig. 4b. The three values of the stretch ratio in Fig. 4 are comparable for both specimens and indicate that the simple uniform compression is approximately applicable to the deformation of the surrounding tissue, and the stretch of the blood vessel is thought to be governed by that of the surrounding tissue.

The stretch ratio at which the thin blood vessels ruptured and the relationship between the stretch ratio and contact force for specimen #200526-05 differed from those for specimen #201109-01. The reason for this difference was unclear at this stage of the study. The stretch ratio at which the thin blood vessels ruptured may vary depending on the variation of the strength of the blood vessel. The deformation of the surrounding tissue is thought to be affected by the original thickness of the loaded part and the mechanical properties of the tissue varying among the specimens.

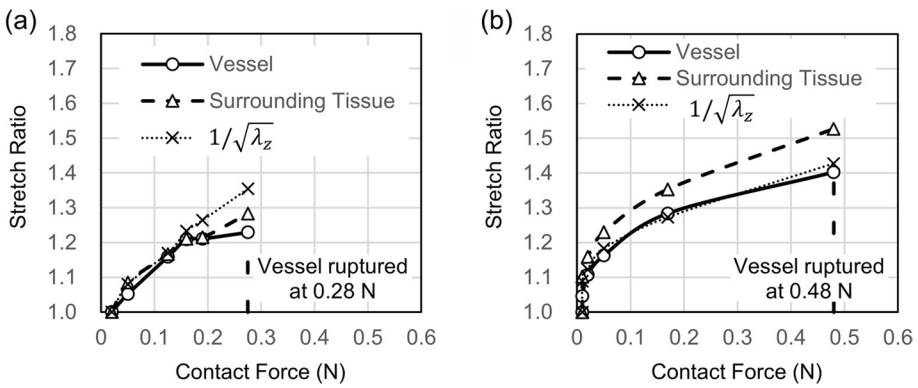

Fig. 4 Stretch ratio of thin blood vessels (circle), surrounding tissues (up-pointing triangle), and $1/\sqrt{\lambda_z}$ (X) for specimens **a** #200526-05 and **b** #201109-01, where λ_z is the ratio of compression of the surrounding tissue in the direction of the contact force

Discussion

Frequency of rupture

The rupture of thin blood vessels was observed in only 2 of the 25 specimens. The low frequency of the observed ruptures was reasonable, which is explained as follows:

(1) Thin blood vessels tend to be invisible under high contact force, despite in vivo staining. Therefore, thin blood vessels may have ruptured under invisible conditions.
(2) The increase in the contact force during the experiments was stopped when all thin blood vessels became invisible. Therefore, some of the experiments may have ended before the contact force caused the rupture of thin blood vessels.
(3) Thin blood vessels outside the depth of field of the microscope were not identified during the experiments. Therefore, thin blood vessels may have ruptured outside the depth of field.
(4) Thin blood vessels outside the view of the microscope were not identified during the experiments. Therefore, thin blood vessels may have ruptured outside the view.

Limitations of this study

This study has the following limitations:

(1) The experiments demonstrated the rupturing process of thin blood vessels, which was discerned using the method developed by Fujikawa and Yamada [21]. Other processes, which were not observed in this study, may also have occurred. For example, if thin blood vessels may have been ruptured in the radial direction, the process would be difficult to detect as the contours of the vessels visualized by this method may not change due to rupturing.
(2) Human tissue was not used in the experiments because the method used in this study is not applicable to human tissue, which is not transparent. A careful comparison between the mechanical properties of the fish and human tissues is needed to apply the results of this study to human injury research. Although the rupturing of fish tissue is thought to be qualitatively similar to that of human tissue, the quantitative data, i.e., the stretch ratio of a thin blood vessel and surrounding tissue and the contact force at the rupture of the vessel, differ between fish and humans. The values for humans should be estimated by simulating the process clarified in this study using the mechanical properties of human tissue.
(3) Although the blood vessels observed in this study were thin, as shown in Figs. 1 and 2, thinner vessels, specifically capillaries, were not examined because they disappeared under the action of a contact force. The structure of capillaries differs from that of other vessels. Therefore, further studies investigating the effects of these differences are required.
(4) The experiments conducted in this study demonstrated the rupturing of thin blood vessels caused by quasi-static contact with blunt objects. Further studies on

dynamic contact may provide better information for discussing human injuries caused by blunt contact in the real world, where dynamic impact may occur.

Rupturing process of thin blood vessels

Blood vessels are made of collagen and elastin, which are elastomers [13, 22]. Although the strength of soft tissue made of collagen and elastin is reinforced by nonuniform microstructures, unlike for other elastomers [23], we assumed that blood vessels rupture under tensile conditions similarly to other elastomers rather than metals or ceramics because they rupture after extremely large elastic deformation similarly to other elastomers [24]. Gent [25] pointed out that this circumstance could occur even when the applied force is compressive. Medri and Strozzi [26] demonstrated a practical example in which an elastomer seal under compression ruptured in a region where the local tensile stress increased. Shmidt [27] reported that the maximum principal stretch ratio represented the strength of a specific elastomer, regardless of the state of deformation. Based on this knowledge, how the local stretch ratio of thin blood vessels reaches the rupturing condition upon the action of compressive contact force during blunt impact is discussed here.

Despite the limitations mentioned above, the results of the experiments indicate one of the rupturing processes of the thin blood vessels under the action of a compressive contact force, as illustrated in Fig. 5. The left-hand-side image in Fig. 5 shows a thin blood vessel in the surrounding tissue without the action of contact force, which is captured in Fig. 3a. As illustrated in the right-hand-side image in Fig. 5, the surrounding tissue is extended in the plane perpendicular to the compressive contact force. Subsequently, the thin blood vessel is pulled into a straight configuration and stretched in the axial direction. Camasão and Mantovani [28] stated that the force "due to the tethering of the vessel with the surrounding tissue at the ends and at several locations along its length" acts on the vessels during deformation. The extension of the surrounding tissue and the vessels is depicted in Fig. 3c. The extension is increased by an additional increase in the contact force, as displayed in Fig. 3c–f. The results that in Fig. 4 indicate that the deformation of the blood vessel is strongly affected by that of the surrounding tissue due to the tethering as Camasão and Mantovani [28] stated. Finally, it ruptures following the process shown in Additional files

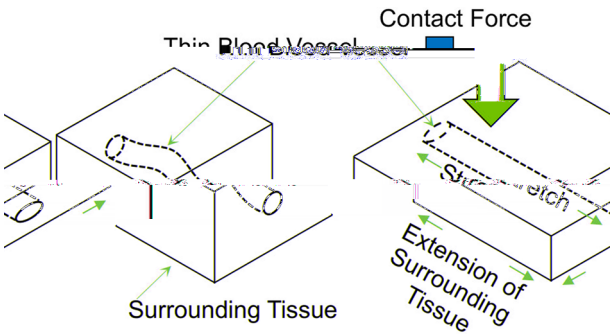

Fig. 5 Stretching modes of the thin blood vessel in the surrounding tissue under the action of compressive contact force

1 and 2 and Figs. 1 and 2. Although the results did not directly provide the thresholds of mechanical inputs for bruising, they indicated that the extension of the surrounding tissue in the direction perpendicular to the contact force as well as the extension of the blood vessels are important factors in bruise formation, which must be reproduced using FEM simulations to determine the thresholds of mechanical inputs for bruising.

The simulation method should be as follows: create a model in which curved, thin blood vessels and the surrounding tissue are placed inside the shape of the target human body part. The blood vessels should be tethered at several locations in the model so that they straighten owing to the extension of the surrounding tissue and then elongate. Calculate the contact force, stress, and strain of the blood vessel and surrounding tissue during impact using an indenter with increasing dynamic indentation. The threshold for the bruise is defined as the contact force when the strain of the blood vessel reaches its ultimate value, which corresponds to the stretch ratio at break. The threshold of the contact pressure is estimated as the normal stress at the interface between the indenter and body part. The threshold of the energy density is evaluated by integrating the contact pressure with respect to the indentation from the start of the contact to the indentation at which the strain of the blood vessel reaches its ultimate value. To implement this, the mechanical properties of the blood vessels and surrounding tissue, i.e., the elastic modules and the stretch ratio at break of the blood vessels and the elastic modules of surrounding tissue, are required. Although several reports [29] exist on the elastic modules of surrounding tissue, future research is required to determine the elastic modules and the stretch ratio at break of blood vessels because the data are limited [24].

Results of experiments in which rapture was not observed

Although the rupture of thin blood vessels was not observed in 23 of the 25 specimens, the following information was obtained from nineteen specimens where the blood vessels were adequately visualized. The thin blood vessels were pulled into straighter configurations during the contact, and the surrounding tissue was extended in the plane perpendicular to the compressive contact force. Additionally, in six specimens where the specific points on the thin blood vessels were identified, axial extension of the vessels due to increasing contact force was observed. The results validate the deformation process illustrated in Fig. 5.

Conclusion

One of the rupturing processes of thin blood vessels under compressive contact force was visualized. The results of this study emphasize that the extension of the surrounding tissue in the plane perpendicular to the contact force plays an essential role in the bruising mechanism because it governs the stretching of thin blood vessels. Since the results do not directly provide, the thresholds of mechanical inputs for bruising, such as contact force, pressure, and impact energy, these should be determined by further research using FEM simulations reproducing the process of deformation and rupture of thin blood vessels, which were visualized in this study.

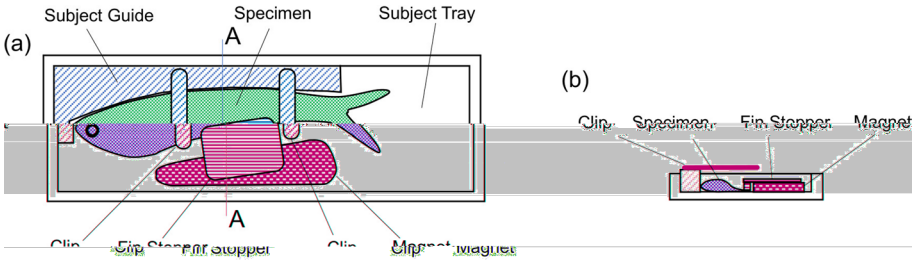

Fig. 6 Subject tray. **a** General view and **b** cross-section along line A–A

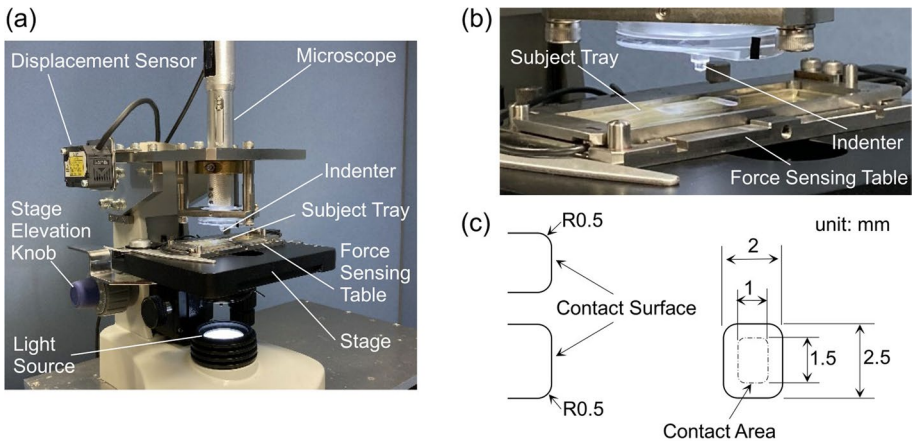

Fig. 7 Microscopic observation apparatus. **a** General view, **b** contacting part, and **c** design of the indenter

Materials and methods

Preparation of specimens

A total of 25 full-grown transparent glass catfish weighing 0.3–1.2 g (mean, 0.7 g) with a length of 42–66 mm (mean, 54 mm) were subjected to the experiments.

The fish were anesthetized by immersing them in buffered MS-222 at a concentration of 75–100 mg/L and fixed on a subject tray. Before the indentation experiments, a dye was injected into the caudal vein of the fish using a glass capillary with an inner diameter of 10 μm. The type, concentration, and amount of the dye varied among the fish because a standard in vivo staining technique for fish blood vessels has not been established. Evans Blue at a concentration of 3–10 mg/mL or eosin at a concentration of 1–10 mg/mL was used as the dye. The injected amount of the dye ranged from 1 to 6 μL/gBW.

Apparatus

A fish was placed on its side on the subject tray and positioned using a subject guide and clips, as shown in Fig. 6a, such that the central part of the caudal region of the fish was between the two clips. The movement of the fish was restricted by a fin stopper, which pressed the anal fin on the subject tray by magnetic force, as shown in Fig. 6b. The subject tray was fixed on a force-sensing table mounted on the stage of the microscopic investigation apparatus, as shown in Fig. 7. The indenter was loaded onto the lateral side of the caudal region of the fish by lifting the stage when the stage elevation knob was

manually rotated. Blood vessels and surrounding tissues were examined through a transparent indenter using a microscope equipped with a video camera (MSBTVTY, 3R Solution Corp., Japan). The indentation was monitored using a laser displacement sensor as the table was displaced. The contact force was measured using a force-sensing table. The indenter was made of transparent acrylic and had a rectangular contact area with dimensions of 1.0 mm × 1.5 mm, as shown in Fig. 7c, which were matched to the field of view of the video camera. The edges of the contact area were rounded with a radius of 0.5 mm to mitigate stress concentration during contact.

In vivo investigation of the blood vessels and surrounding tissue

The subject tray containing the fish was filled with buffered MS-222 (75–100 mg/L). The horizontal position of the microscope stage was adjusted such that the indenter contacted the area between the hemal spines in the caudal region of the fish. A live view of the blood vessels and surrounding tissues was displayed on a personal computer connected to the microscope and recorded as a movie. First, the stage was gradually lifted to increase the contact force. The gradual loading in this experiment represents the quasi-static contact between a blunt moving part and the live soft tissues in the real world. Next, the increase of the contact force was stopped when one of the following three conditions was satisfied: (1) when it exceeded 4 N, at which a bone contusion had affected the investigation in a previous study [21], (2) when the rupture of the blood vessels was observed, or (3) when the blood vessels became invisible. Finally, the table was lowered to release the contact. After the investigation, the fish were euthanised by immersing them in buffered MS-222 at a concentration of 500 mg/L.

Stretch ratio of thin blood vessels and surrounding tissues

The stretch ratio λ_{xj} of the thin blood vessel and the surrounding tissue in the plane perpendicular to the contact force was calculated using the following formula:

$$\lambda_{xj} = e^{\varepsilon_j}, \tag{2}$$

$$\varepsilon_j = \sum_{k=1}^{j} \Delta\varepsilon_k, \tag{3}$$

$$\Delta\varepsilon_k = \ln\left(l_k / l_{k-1}\right), \tag{4}$$

where the indices j and k denote the steps of the calculation starting with 0 at the initial condition; ε_j is the true tensile strain; $\Delta\varepsilon_k$ is the incremental strain; and l_k is the distance between the specific parts of the thin blood vessel or the surrounding tissue in the plane perpendicular to the contact force. l_k is measured in the microscopic movie by tracking specific points.

Supplementary Information

The online version contains supplementary material available at https://doi.org/10.1186/s12938-024-01284-2.

Additional file 1. Tensile rupture of the thin blood vessel. The movie file in which the rupturing vessel is observed in specimen #200526-05 at a contact force of 0.28 N.

Additional file 2. Tensile rupture of the thin blood vessel. The movie file in which the rupturing vessel is observed in specimen #201109-01 at a contact force of 0.48 N.

Additional file 3. Deformation of the thin blood vessel and the surrounding tissue in specimen #200526-05.

Additional file 4. Deformation of the thin blood vessel and the surrounding tissue in specimen #201109-01.

Acknowledgements
The authors thank Dr. Ken Watanabe from National Center for Geriatrics and Gerontology for advice on experimental design.

Author contributions
TF developed the experimental procedures, performed them, and analyzed the data. YY contributed primarily to designing the study and interpreting the results. All the authors read and approved the final manuscript. T.F. and Y.Y. wrote the main manuscript text. T.F. prepared figures. All authors reviewed the manuscript.

Funding
This research was conducted as part of the "International Standardisation on Measurement Methods of Skin Injury Tolerance for Next-generation Safety of Machinery in Human–machine Interaction" by the Ministry of Economy, Trade, and Industry of Japan.

Availability of data and materials
The movie files recorded in this study are available from the public repository Zenodo (https://zenodo.org/record/8194902).

Declarations

Ethics approval and consent to participate
This study was approved by the Nagoya University Animal Care and Use Committee (No. ENG20-2) and performed in accordance with the Nagoya University Regulations on Animal Care and Use in Research.

Consent for publication
Not applicable.

Competing interests
The authors declare that they have no competing interests. No benefits in any form have been or will be received from any commercial party directly or indirectly related to the research conducted in this manuscript.

Received: 17 June 2024 Accepted: 27 August 2024
Published online: 11 September 2024

References

1. Haddadin S, Haddadin S, Khoury A, Rokahr T, Parusel S, Burgkart R, Albu-Schäffer A. On making robots understand safety: embedding injury knowledge into control. Int J Robot Res. 2012;31(13):1578–602. https://doi.org/10.1177/0278364912462256.
2. Povse B, Haddadin S, Belder R, Koritnik D, Bajd T. A tool for the evaluation of human lower arm injury: approach, experimental validation and application to safe robotics. Robotica. 2016;34(11):2499–515. https://doi.org/10.1017/S0263574715000156.
3. Behrens R, Pliske G, Piatek S, Walcher F, Elkmann N. A statistical model to predict the occurrence of blunt impact injuries on the human hand–arm system. J Biomech. 2023;151: 111517. https://doi.org/10.1016/j.jbiomech.2023.111517.
4. Black HI, Coupaud S, Daéid NN, Riches PE. On the relationships between applied force, photography technique, and the quantification of bruise appearance. Forensic Sci Int. 2019;305: 109998. https://doi.org/10.1016/j.forsciint.2019.109998.
5. Desmoulin GT, Anderson GS. Method to investigate contusion mechanics in living humans. J Forensic Biomech. 2011;2: F100402. https://doi.org/10.4303/jfb/F100402.
6. Langlois NEI, Gresham GA. The ageing of bruises: a review and study of the colour changes with time. Forensic Sci Int. 1991;50(2):227–38. https://doi.org/10.1016/0379-0738(91)90154-B.
7. Vanezis P. Interpreting bruises at necropsy. J Clin Pathol. 2001;54(5):348–55. https://doi.org/10.1136/jcp.54.5.348.
8. Huang L, Bakker N, Kim J, Marston J, Grosse I, Tis J, Cullinane D. A multi-scale finite element model of bruising in soft connective tissues. J Forensic Biomech. 2012;3:1–5. https://doi.org/10.4303/jfb/235579.
9. Tang K, Sharpe W, Schulz A, Tam E, Grosse I, Tis J, Cullinane D. Determining bruise etiology in muscle tissue using finite element analysis. J Forensic Sci. 2014;59(2):371–4. https://doi.org/10.1111/1556-4029.12349.
10. Grosse IR, Huang L, Davis JL, Cullinane D. A multilevel hierarchical finite element model for capillary failure in soft tissue. J Biomech Eng. 2014;136(8): 081010. https://doi.org/10.1115/1.4027730.
11. Higuchi Y, Fujikawa T, Sugiura R, Nishimoto T, Sato F. Development of a porcine thigh finite element model for evaluating the soft-tissue injuries caused by blunt impacts during human–robot interactions. In: 2021 IEEE international

conference on intelligence and safety for robotics (ISR). 2021. p. 301–5. https://doi.org/10.1109/ISR50024.2021.9419540.
12. Spilsbury B. The medico-legal significance of bruises. Medicao-Legal Criminol Rev. 1939;7(3):215–27. https://doi.org/10.1177/030216373900700302.
13. West JB, Mathieu-Costello O. Stress failure of pulmonary capillaries as a limiting factor for maximal exercise. Eur J Appl Physiol. 1995;70:99–108. https://doi.org/10.1007/BF00361536.
14. Deane M, Gregory M, Mars M. The effect of a contusion injury on rabbit skeletal muscle: a morphological study. Open Access J Sci Technol. 2013;1(3):1–8. https://doi.org/10.11131/2013/100012.
15. Barington K, Jensen HE. The impact of force on the timing of bruises evaluated in a porcine model. J Forensic Legal Med. 2016;40:61–6. https://doi.org/10.1016/j.jflm.2016.03.005.
16. Fujikawa T, Sugiura R, Nishikata R, Nishimoto, T. Critical contact pressure and transferred energy for soft tissue injury by blunt impact in human–robot interaction. In: 2017 17th international conference on control, automation and systems (ICCAS). 2017. p. 867–72. https://doi.org/10.23919/ICCAS.2017.8204347.
17. Fujikawa T, Sugiura, R, Nishikata R, Yamada Y, Nishimoto T. Marmarou-type impact tests to investigate criteria for avoiding bruises in extremities by human–robot contact. In: 2021 IEEE international conference on intelligence and safety for robotics (ISR). 2021. p. 297–300. https://doi.org/10.1109/ISR50024.2021.9419547.
18. Rishpon A, Kim N, Scope A, Porges L, Oliviero MC, Braun RP, Marghoob AA, Fox CA, Rabinovitz HS. Reflectance confocal microscopy criteria for squamous cell carcinomas and actinic keratoses. Arch Dermatol. 2009;145(7):766–72. https://doi.org/10.1001/archdermatol.2009.134.
19. Watanabe K, Nishimura Y, Nomoto T, Umemoto N, Zhang Z, Zhang B, Kuroyanagi J, Shimada Y, Shintou T, Okano M, Miyazaki T, Imamura T, Tanaka T. In vivo assessment of the permeability of the blood–brain barrier and blood–retinal barrier to fluorescent indoline derivatives in zebrafish. BMC Neurosci. 2012;13:101. https://doi.org/10.1186/1471-2202-13-101.
20. Steffensen JF, Lomholt JP, Vogel WOP. In vivo observations on a specialized microvasculature, the primary and secondary vessels in fishes. Acta Zool. 1986;67(4):193–200. https://doi.org/10.1111/j.1463-6395.1986.tb00863.x.
21. Fujikawa T, Yamada Y. Novel in-vivo microscopy technique for internal bleeding using transparent fish. In: 2021 IEEE international conference on intelligence and safety for robotics (ISR). 2021. p. 306–309. https://doi.org/10.1109/ISR50024.2021.9419514.
22. Shadwick RE. Mechanical design in arteries. J Exp Biol. 1999;202(23):3305–13. https://doi.org/10.1242/jeb.202.23.3305.
23. Yang W, Sherman VR, Gludovatz B, Schaible E, Stewart P, Ritchie RO, et al. On the tear resistance of skin. Nat Commun. 2015;6:6649. https://doi.org/10.1038/ncomms7649.
24. Suh C-M, Kim S-H, Monson KL, Goldsmith W. Tensile characteristics and behavior of blood vessels from human brain in uniaxial tensile test. KSME Int J. 2003;17:1016–25. https://doi.org/10.1007/BF02982986.
25. Gent AN, Mars WV. Strength of elastomers. In: Erman B, Mark JE, Roland CM, editors. The science and technology of rubber. 4th ed. New York: Academic Press; 2013. p. 473–516. ISBN: 978-0-12-394584-6.
26. Medri G, Strozzi A. Stress–strain fields in compressed elastomeric seals and their extension to fracture mechanics. Rubber Chem Technol. 1986;59(5):709–21. https://doi.org/10.5254/1.3538229.
27. Schmidt A, Rothemund P, Mazza E. Multiaxial deformation and failure of acrylic elastomer membranes. Senso Actuators A Phys. 2012;174:133–8. https://doi.org/10.1016/j.sna.2011.12.004.
28. Camasão DB, Mantovani D. The mechanical characterization of blood vessels and their substitutes in the continuous quest for physiological-relevant performances. Crit Rev Mater Today Bio. 2021;10: 100106. https://doi.org/10.1016/j.mtbio.2021.100106.
29. Alkhouli N, Mansfield J, Green E, Bell J, Knight B, Liversedge N, et al. The mechanical properties of human adipose tissues and their relationships to the structure and composition of the extracellular matrix. Am J Physiol Endocrinol Metab. 2013;305(12):E1427–35. https://doi.org/10.1152/ajpendo.00111.2013.

Publisher's Note